On-the-fly Symmetrical Quasi-classical Dynamics with Meyer-Miller Mapping Hamiltonian for the Treatment of Nonadiabatic Dynamics at Conical Intersections

Deping Hu[†‡°], *Yu Xie*[†‡°], *Jiawei Peng*[†‡], *Zhenggang Lan*[†‡*]

[†]SCNU Environmental Research Institute, Guangdong Provincial Key Laboratory of Chemical Pollution and Environmental Safety & MOE Key Laboratory of Environmental Theoretical Chemistry, South China Normal University, Guangzhou 510006, China

[‡]School of Environment, South China Normal University, Guangzhou 510006, China

KEYWORDS: Meyer-Miller model, on the fly, quasi-classical dynamics, nonadiabatic dynamics, conical intersection

Abstract

The ‘on-the-fly’ version of the symmetrical quasi-classical dynamics method based on the Meyer-Miller mapping Hamiltonian (SQC/MM) is implemented to study the nonadiabatic dynamics at conical intersections of polyatomic systems. The current ‘on-the-fly’ implementation of the SQC/MM method is based on the adiabatic representation and the dressed momentum. To include the zero-point energy (ZPE) correction of the electronic mapping variables, we employed both the γ-adjusted and γ-fixed approaches. Nonadiabatic dynamics of the methaniminium cation ($CH_2NH_2^+$) and azomethane are simulated using the on-the-fly SQC/MM method. For $CH_2NH_2^+$, both two ZPE correction approaches give reasonable and consistent results. However, for azomethane, the γ-adjusted version of the SQC/MM dynamics behaves much better than the γ-fixed version. The further analysis indicates that it is always recommended to use the γ-adjusted SQC/MM dynamics in the on-the-fly simulation of photoinduced dynamics of polyatomic systems, particularly when the excited-state is well separated from the ground state in the Frank-Condon region. This work indicates that the on-the-fly SQC/MM method is a powerful simulation protocol to deal with the nonadiabatic dynamics of realistic polyatomic systems.

1. Introduction

The theoretical description of the nonadiabatic dynamics at conical intersections (CIs) in complex systems always arouses great research interests due to the breaking down of the Born-Oppenheimer (BO) approximation and the involvement of a large number of degrees of freedom (DoFs).[1-3] Various theoretical approaches were developed to simulate the nonadiabatic dynamics,[1-10] which for example include the full quantum dynamics[2,11-15] and different versions of mixed quantum-classical/semi-classical dynamics.[1-2,5-6,8-10,16-26] The complex potential energy functions of the polyatomic molecules with many DoFs impose some additional challenging in the simulation of the nonadiabatic dynamics. To solve such problems, the combination of on-the-fly simulation with various dynamics methods becomes popular in the simulation of the real-time nonadiabatic dynamics of polyatomic systems at all atomic level.[5-6,9-10,21,27]

Because the electronic structure calculations are generally performed at each time step in the on-the-fly dynamics, the total cost of on-the-fly simulation is rather high. For this reason, on-the-fly simulation of the nonadiabatic dynamics should normally employ practical dynamical methods that can provide a good balance between computational cost and efficiency. Thus, only a few dynamical approaches are possible choices. For example, trajectory surface hopping (TSH) approaches, such as the Tully's fewest switch surface hopping (FSSH) approach and its extension,[18,20] Landau-Zener/Zhu-Nakamura surface hopping approaches,[24,28] were employed in the on-the-fly simulation due to their computational efficiency. In recent years, great progress was made to use Tully's on-the-fly FSSH (and its variations) dynamics to treat the nonadiabatic

dynamics of realistic polyatomic systems.[2,9,21,27] However, the improper treatment of electronic coherence and frustrated hops in Tully's FSSH approach were widely discussed.[8,19-20,29] Recent work also tried to combine a more rigorous surface hopping approach[30] in on-the-fly simulation, which is derived from the exact factorization of the electronic-nuclear wavefunction.[31] Considerable efforts were made to combine the on-the-fly simulation with the Gaussian-wavepacket based and relevant approaches,[5,10,32-33] such as the ab initio multiple spawning (AIMS),[5,10] variational multiconfigurational Gaussians (vMCG)[32] and multiconfigurational Ehrenfest.[34] Some numerical details should be concerned in the implementation of these approaches. For instance, the new Gaussian wave-packets[10] should be properly generated in the AIMS and reasonable basis-function sampling/cloning should be considered in the multiconfigurational Ehrenfest dynamics.[35] These approaches are very promising because these theoretical frameworks were more rigorous and the computational cost is reasonable.

As expected, only the dynamical approaches with reasonable computational cost may be suitable for on-the-fly dynamics. Particularly, the methods based on the independent trajectories, instead of entangled trajectories, are preferred in the implementation of on-the-fly simulation if both require a similar number of trajectories. According to this idea, it is clear that the symmetrical quasi-classical dynamics based on the Meyer-Miller mapping Hamiltonian (SQC/MM)[36-38] may be an alternative and suitable approach for on-the-fly simulation. In the Meyer-Miller (MM) mapping model,[36] a Hamiltonian with N discrete quantum states is mapped to an effective Hamiltonian (or a mapping Hamiltonian) with N coupled harmonic oscillators.[8,36,39-40] It is possible

to combine the MM mapping Hamiltonian with different dynamics approaches, such as various quasi-classical/semi-classical dynamics approaches,[41-49] quantum-classical Liouville equation (QCLE),[50-53] path integral and extension,[54-59] surface hopping,[60-61] centroid molecular dynamics (CMD),[62] and ring-polymer molecular dynamics (RPMD).[63-69] In the quasi-classical dynamics, the inclusion of the zero-point energy (ZPE) in the electronic mapping variables in principle provides better dynamical results than the Ehrenfest dynamics,[36] while the partial instead of full ZPE should be included in practice.[8,70-72] When the 'bin' technique is taken to perform the initial sampling and the final assignment of the quantum states, the SQC/MM[38,73] is formulated.

The SQC/MM method gained significant attention due to its numerical simplicity and physical insight.[38,73-90] The reasonable performance of the SQC/MM dynamics was examined by different benchmark works.[47,81-82,86-87,89] Within the framework of the SQC/MM dynamics, Cotton and Miller suggested different useful approaches in the implementation, such as the triangle windowing technique[80,91] and the employment of the trajectory-adjusted electronic ZPE correction[92] in the SQC/MM approach. The SQC/MM method was employed to treat different types of nonadiabatic dynamics,[38,73,81-86,93] for example excited-state energy/electronic transfer dynamics,[73,81,86,90,93] singlet fission[83-85] and scattering dynamics[82] and photo-dissociation dynamics.[92] Overall, the SQC/MM method is very promising, thus it is highly interesting to introduce it into on-the-fly dynamics for all-atomic simulation of the nonadiabatic dynamics of polyatomic molecules in real time.

Recently, Huo and coworkers proposed to employ the quasi-diabatization procedure in the

dynamics propagation.[88,94-97] They used the quasi-diabatic basis to propagate the MM mapping Hamiltonian based dynamics such as partial-linearized density matrix (PLDM) path-integral approach and SQC/MM approach. Particularly, they made the initial efforts to combine the PLDM path-integral approach, the classical path approximation, and density functional tight-binding (DFTB) calculations to achieve the on-the-fly simulation of nonadiabatic dynamics of photoinduced charge transfer in organic photovoltaic systems.[95] Late, they extended their approach to study the photoinduced dynamics at CIs.[97] The quasi-diabatic approach works quite well and improves numerical stability in several cases. When the electronic states involved in the nonadiabatic dynamics have non-neglectable couplings with the higher electronic states, the curl condition is not satisfied.[1,98-101] In this case, it is not trivial to construct the quasi-diabatic electronic basis within the subspace spanned by a few electronic states, unless a much larger number of electronic states are considered in the adiabatic-to-diabatic transformation. The inclusion of many electronic states may bring some additional challenging in the high-level electronic-structure calculations. Alternatively, it is also possible to formulate the MM mapping Hamiltonian in the adiabatic representation,[36,56,75,102-104] providing a natural interface to combine the electronic structure calculations. Along this road, Miller and coworkers[75] recently re-formulated the SQC/MM dynamics in the adiabatic representation by using the dressed momentum, namely *kinematic* momentum. This formulism provides us an important starting point for the implementation of on-the-fly SQC/MM dynamics. We noticed that Cui and coworkers tried to combine this approach with the on-the-fly simulation using the semi-empirical electronic-structure

calculations.[105] This work also shows that the on-the-fly SQC/MM dynamics results are sensitive with the choice of the window width and ZPE correction parameter γ when γ is fixed in the SQC/MM dynamics. In fact, the possible influence of the window width on the dynamics was also discussed in several previous works.[77,80] This problem may be partially remedied by the trajectory-adjusted electronic ZPE approach proposed by Cotton and Miller.[92] Thus, in principle, this γ-adjusted approach is highly recommended in the on-the-fly SQC/MM dynamics to study the photochemistry of realistic systems.

In this work, we try to combine the SQC/MM method with the on-the-fly dynamics. To know more about the performance of the SQC/MM method in on-the-fly nonadiabatic dynamics compared with other methods, such as FSSH and AIMS, two commonly used molecular systems, methaniminium cation ($CH2NH2^+$) and azomethane, were chosen in this work. Since we noticed that the choice of the ZPE correction in the SQC/MM dynamics is not a trivial task, we implemented both the γ-fixed and γ-adjusted approaches. In the latter case, the γ is determined by the initial condition of the electronic DoF for each trajectory. This combination provides a novel simulation tool to describe the full-dimensional nonadiabatic dynamics at CIs of polyatomic systems. All implementation is performed based on the nonadiabatic dynamics simulation package JADE developed in our group.[106-107] In this sense, we also largely extend the JADE code to allow the on-the-fly dynamics simulation of nonadiabatic dynamics at CIs with various dynamics approaches.

2. Theory and Methods

2.1. SQC/MM Hamiltonian on the adiabatic representation

The adiabatic representation of MM Hamiltonian can be written as[75]

$$H = \frac{1}{2\mathbf{M}}\mathbf{P}_{\text{kin}}^2 + \sum_i^F \left(\frac{1}{2} x_i^{\,2} + \frac{1}{2} p_i^{\,2} - \gamma \right) E_i\left(\mathbf{R}\right) \tag{1}$$

with the *kinematic* momentum $\mathbf{P}_{\text{kin}}$ defined as

$$\mathbf{P}_{\text{kin}} = \mathbf{P} + \sum_{i \neq j} x_i p_j \mathbf{d}_{ij}\left(\mathbf{R}\right) \tag{2}$$

where (**R**, **P**) are the coordinates and momenta of the nuclear DOFs, F is the number of electronic states, (x_i, p_i) is the coordinate and momentum of the harmonic oscillator that maps to the i-th electronic state, $E_i\left(\mathbf{R}\right)$ denotes the energy of the i-th electronic state, γ represents the ZPE correction parameter and $\mathbf{d}_{ij}\left(\mathbf{R}\right)$ is the first-order nonadiabatic coupling (NAC) vector.

Previous work demonstrated that replacement of the effective potential term in Eq. (1),

$$V_{eff} = \sum_i^F \left(\frac{1}{2} x_i^{\,2} + \frac{1}{2} p_i^{\,2} - \gamma \right) E_i\left(\mathbf{R}\right) \tag{3}$$

by a symmetrized one

$$V_{eff} = \frac{1}{F}\sum_i^F E_i\left(\mathbf{R}\right) + \frac{1}{F}\sum_{ij}^F \frac{1}{2}\left(n_i - n_j\right)\left(E_i\left(\mathbf{R}\right) - E_j\left(\mathbf{R}\right)\right) \tag{4}$$

in the propagation generally gives better dynamics results,[82] where

$$n_i = \frac{1}{2} x_i^{\,2} + \frac{1}{2} p_i^{\,2} - \gamma \tag{5}$$

is the action variable for the i-th electronic state. Therefore, our current on-the-fly implementation used the following equation of motions (EOMs)

$$
\begin{aligned}
\frac{dx_i}{dt} &= p_i \frac{1}{F}\sum_j^F \Big(E_i(\mathbf{R}) - E_j(\mathbf{R})\Big) + \sum_j x_j \mathbf{d}_{ji}(\mathbf{R}) \cdot \frac{\mathbf{P}_{\text{kin}}}{\mathbf{M}} \\
\frac{dp_i}{dt} &= -x_i \frac{1}{F}\sum_j^F \Big(E_i(\mathbf{R}) - E_j(\mathbf{R})\Big) + \sum_j p_j \mathbf{d}_{ji}(\mathbf{R}) \cdot \frac{\mathbf{P}_{\text{kin}}}{\mathbf{M}} \\
\frac{d\mathbf{R}}{dt} &= \frac{\mathbf{P}_{\text{kin}}}{\mathbf{M}} \\
\frac{d\mathbf{P}_{\text{kin}}}{dt} &= -\frac{\partial V_{\text{eff}}}{\partial \mathbf{R}} - \frac{1}{2}\sum_{ij}\Big(x_i x_j + p_i p_j\Big)\Big(E_j(\mathbf{R}) - E_i(\mathbf{R})\Big)\mathbf{d}_{ij}(\mathbf{R})
\end{aligned}
\tag{6}
$$

2.2. Symmetrical triangle window and initial sampling

In the SQC/MM dynamics, the "window function" was both used for the initial sampling of the electronic DOF and final assignment for the quantum state. The triangle window function[91] for multistate used in this work is defined as below

$$
W_i(\mathbf{n} = n_1, \ldots n_i, \ldots n_f) = w_1(n_i) \cdot \prod_{i \neq j}^{\text{F}} w_0(n_i, n_j) \tag{7}
$$

with

$$
w_1(n_i) = \begin{cases} (2 - \gamma - n_i)^{2-\text{F}} & \text{for } 1 - \gamma < n_i < 2 - \gamma \\ 0 & \text{otherwise,} \end{cases} \tag{8}
$$

and

$$
w_0(n_i, n_j) = \begin{cases} 1 & \text{for } n_j < 2 - 2\gamma - n_i \\ 0 & \text{otherwise.} \end{cases} \tag{9}
$$

The system is regarded as staying at the *i*-th electronic state if $W_i = 1$ at any moment along the trajectory.

The action-angle sampling method was used to generate the initial x_i^0 and p_i^0 for the *i*-th electronic state, which is

$$x_i^0 = \sqrt{2(n_i^0 + \gamma)}\cos\theta$$
$$p_i^0 = \sqrt{2(n_i^0 + \gamma)}\sin\theta, \tag{10}$$

where n_i^0 is sampled according to the triangle function and $\theta \in [-\pi, \pi]$. The final assignment is performed by binning the action variables into the corresponding windows. In the γ-fixed approach, this γ value is determined by the triangle window function.[91]

2.3. Trajectory-adjusted electronic ZPE

Recently, Cotton and Miller proposed a ZPE adjustment protocol,[92] which modifies the ZPE correction parameter γ for each trajectory. After the initial sampling according to the triangle window, the coordinate and momentum of the electronic DoF are x_i^0 and p_i^0, respectively. This in fact defines the ZPE for each trajectory, namely

$$\gamma_i = \frac{1}{2}(x_i^0)^2 + \frac{1}{2}(p_i^0)^2 - \delta_{ij} \tag{11}$$

j is the initial adiabatic electronic state used in the sampling process. This indicates that the corresponding ZPE correction parameter γ_i of each trajectory is different. Under this trajectory-adjusted γ_i, the action of electronic DoFs becomes

$$n_i = \frac{1}{2}x_i^2 + \frac{1}{2}p_i^2 - \gamma_i \tag{12}$$

during the trajectory propagation. At the same time, the expression of the MM Hamiltonian in the adiabatic representation should also take the trajectory-adjusted ZPE into account, namely

$$H = \frac{1}{2\mathbf{M}}\mathbf{P}_{\text{kin}}^2 + \sum_i^F \left(\frac{1}{2}x_i^2 + \frac{1}{2}p_i^2 - \gamma_i\right) E_i(\mathbf{R}) \tag{13}$$

In the trajectory propagation, the time-dependent action of the electronic DoFs is calculated

according to Eq. (12). Next, the final assignment of the quantum state is performed according to Eq. (7-9) in which the γ value is replaced by the trajectory-adjusted γ_i of each trajectory. More discussions on the technical details of this trajectory-adjusted electronic ZPE were clearly given in reference.[92]

2.4. Computational details

Both $CH_2NH_2^+$ and azomethane (Scheme 1) were often taken as typical examples to test the direct nonadiabatic dynamics approaches.[30,106-120] Therefore, we also examined their excited state dynamics by using the on-the-fly SQC/MM dynamics. In addition, the FSSH dynamics were also performed.

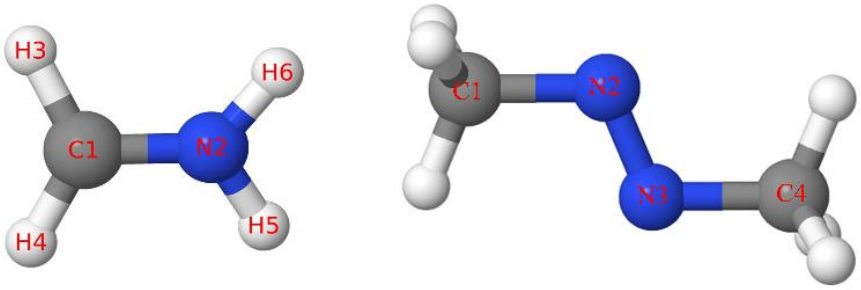

Scheme 1. Chemical structure of $CH_2NH_2^+$ (left) and azomethane (right) with atom labels.

The ground state (S_0) minima were optimized at DFT/B3LYP/6-31G* level using the Gaussian 16 package.[121] The initial sampling of the nuclear coordinates and momenta was performed by the Wigner sampling of the lowest vibrational level on the electronic ground state.

For $CH_2NH_2^+$, we considered the dynamics starting from both the first (S_1) and second (S_2) excited state individually. While for azomethane, we explored the dynamics starting from the S_1 state.

In the SQC/MM dynamics, the initial sampling and final assignment of the quantum state for electronic DoF were performed using the symmetrical triangle window tricks. In the SQC/MM dynamics, both γ-adjusted and γ-fixed approaches were implemented.

In the FSSH dynamics, the trajectories were first directly put in the adiabatic electronic states where dynamics started. The hop probabilities were calculated according to Tully's Fewest switch algorithm.[18] We employed the decoherence correction proposed by Granucci et al. and set the parameter $\alpha = 0.1$.[29]

In both the SQC/MM and FSSH dynamics, the nuclear equations of motion were integrated with time steps, 0.5 and 0.2 fs, respectively. For each step of nuclear motion, 100 steps of electronic motion were performed. The final results were obtained by averaging over 200 trajectories for all dynamics. The convergence with respect to the number of trajectories is given in Appendix.

The values of electronic energies, first-order derivative NACs and gradients can be obtained from the on-the-fly quantum chemistry calculation. In this work, the complete active space self-consistent field (CASSCF) method[122-123] with 6-31G* basis set was used in the electronic structure calculation process. For $CH_2NH_2^+$, three state average with active space of six electrons in orbitals [SA-3-CAS(6,4)] was used in the CASSCF calculation. For azomethane, SA-2-CAS(6,4) was used.

All the dynamics calculations were performed with a development version of the JADE package.[106-107] The CASSCF calculations were performed with the MOLPRO software.[124]

3. Results and Discussion

3.1. CH2NH2+

For $CH2NH2^+$, no matter whether the dynamics starts from S_2 or S_1 state, all selected dynamics approaches basically give consistent results on the time-dependent electronic populations, see Figure 1(a) and (b). Here we take γ-adjusted SQC/MM dynamics as an example. When the dynamics starts from the S_2 state, the system switches from the S_2 state to the S_1 state very rapidly (< 10 fs), as shown in Figure 1(a). At 10 fs, the population in the S_0 state starts to increase. The lifetimes of the S_2 and S_1 states are approximately 9 fs and 30 fs, respectively, consistent with many previous theoretical works.[2,30,106-111,114,117-118]

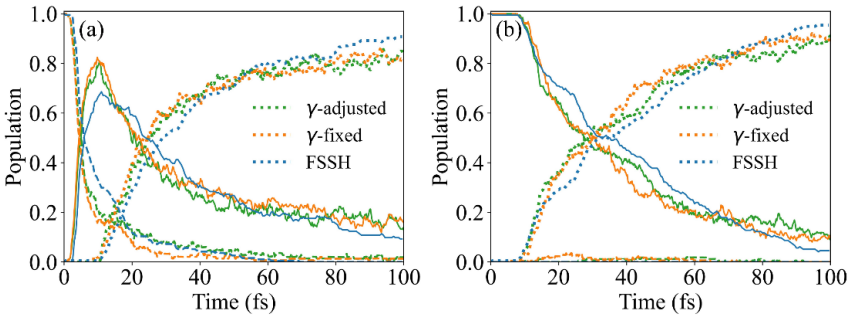

Figure 1. The time-dependent electronic population of S_0 (dotted line), S_1 (solid line) and S_2 (dashed line) states with the initial state of (a) S_2 and (b) S_1. 200 trajectories were used for all dynamics.

It is well known that the CN stretching motion plays an important role in the nonadiabatic decay dynamics of $CH_2NH_2^+$,[106-108,125] when the dynamics starts from the S_2 state. Here we plotted the time-dependent CN distance of a swarm of trajectories in Figure 2. In line with the results of the decay of electronic population, the CN stretching motions are also very similar for all dynamics.

It is obvious that two types of trajectories exist during the dynamical run.

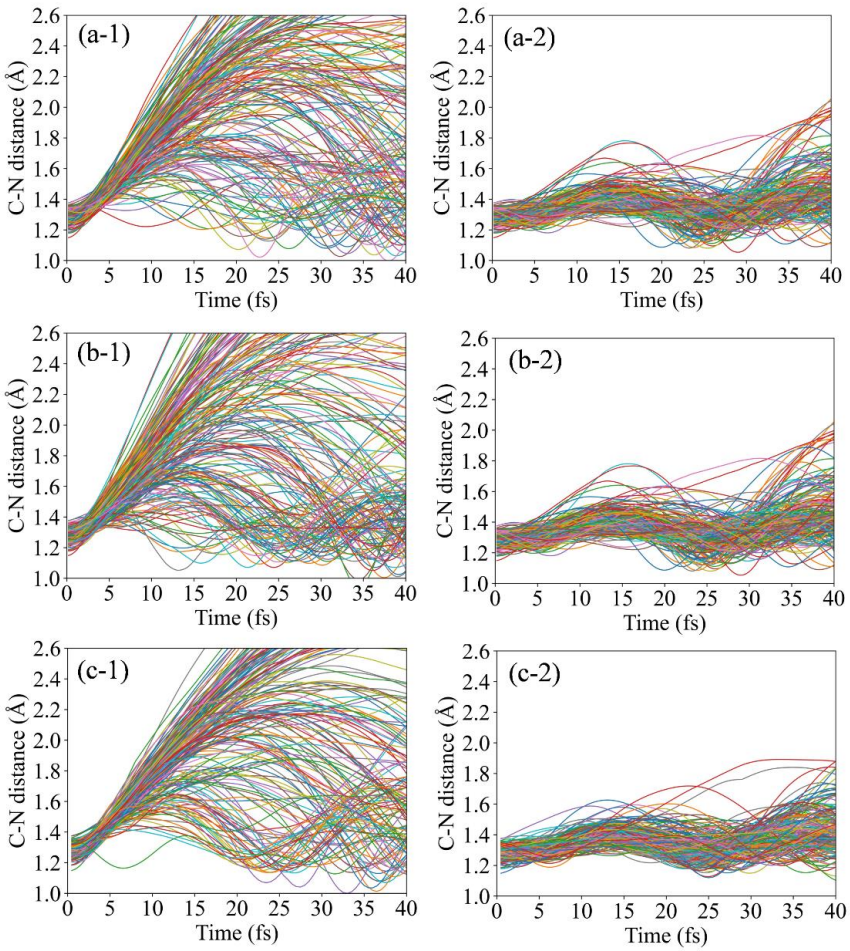

Figure 2. The time-dependent CN distance of $CH_2NH_2^+$ in the (a) γ-adjusted, (b) γ-fixed SQC/MM and (c) FSSH dynamics. The initial states are (1) S_2 and (2) S_1, respectively.

The first group of trajectories displays a significant CN elongation, while for the second group of trajectories, the CN bond only experiences weak oscillation patterns. To understand geometrical features near the S_1/S_0 CI seam, we also examine the distribution of the S_1/S_0 "switching points" in the SQC/MM dynamics, where the S_1/S_0 energy gaps reach the minimum before the S_0 state is occupied along the trajectory propagation, see Figure 3. Here we also provided the geometrical

distribution at the S_1/S_0 hops in the FSSH dynamics. The key role of the CN bond stretching motion is confirmed, while the strong bi-pyramidalization motions at both C and N sites are also important.

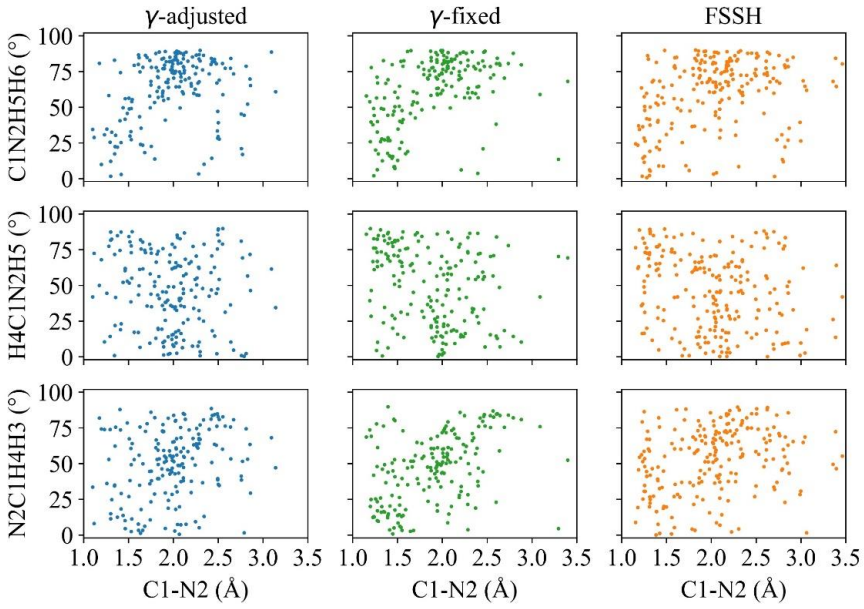

Figure 3. Various dihedral angles versus CN stretching of the $CH_2NH_2^+$ molecule at S_1/S_0 "switching point" with the starting state at the S_2 state: dihedral angle 4-1-2-5 (CN torsion angle), dihedral angle 1-2-5-6 (pyramidalization at N atom) and dihedral angle 2-1-4-3 (pyramidalization at C atom).

For the second group of trajectories that do not show the pounced CN elongation, the molecular motion in the nonadiabatic decay is rather complex, which is characterized by the highly mixed motions of the bi-pyramidalization motions at both C and N sites and the torsional motion of the CN bond, as shown in Figure 3.

Although the dynamics calculated by the three approaches looks not far from each other, some visible differences exist. For instance, the time-dependent populations predicted by two

SQC/MM dynamics are more similar, while slightly different results are obtained in the FSSH method. As the contrast, we notice that the distribution of "switching points" from the γ-adjusted SQC/MM dynamics is more similar to the FSSH dynamics, while different distribution patterns were found in the γ-fixed SQC/MM dynamics.

When the initial state is S_1, the exponential decay of S_1 is observed with a lifetime of ~27 fs, see Figure 1(b). During the whole decay dynamics, the S_2 state is only weakly populated and its influence is neglectable. It is important to notice that the geometrical evolution in this case is quite different with respect to the dynamics starting from the S_2 state. For most trajectories, the CN distance remains relatively short (about 1.2~1.6 Å) during the evolution, see Figure 2. We also noticed that the bi-pyramidalization at both C and N sites, and torsional motion of the CN bond, are responsible for the $S_1 \rightarrow S_0$ decay, as shown in Figure 4.

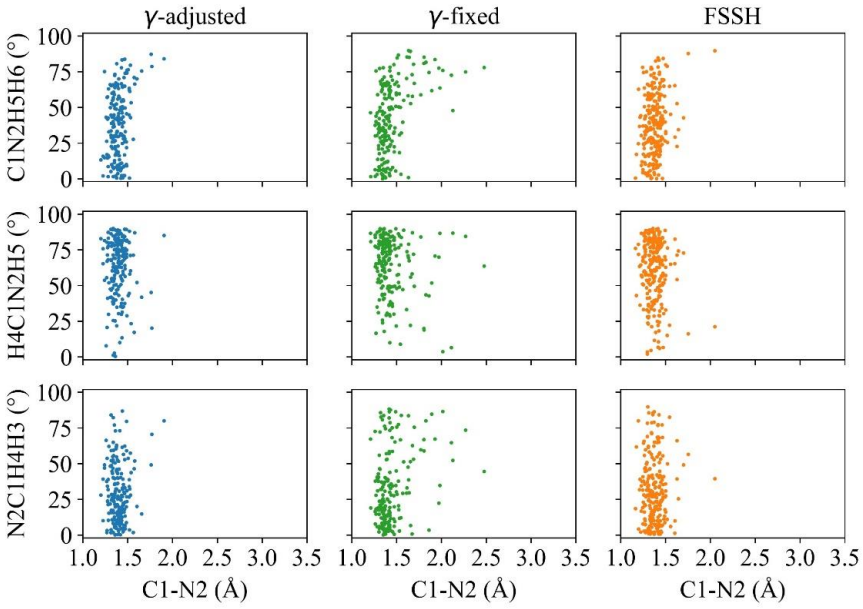

Figure 4. Various dihedral angles versus CN stretching of the $CH_2NH_2^+$ molecule at S_1/S_0

"switching point" with the starting state at the S_1 state: dihedral angle 4-1-2-5 (CN torsion angle), dihedral angle 1-2-5-6 (pyramidalization at N atom) and dihedral angle 2-1-4-3 (pyramidalization at C atom).

No matter whether the dynamics starts from the S_1 or S_2 state, the dynamics features, including excited-state lifetimes, the major reactive molecular motion in the excited-state nonadiabatic dynamics, and the geometrical feature in the relevant CI seam, with different dynamics methods used in this work, the γ-adjusted and γ-fixed SQC/MM dynamics and FSSH, are basically consistent, see Figure 1-4. In addition, the dynamics results are highly consistent with previous on-the-fly studies with various methods, such as the TSH dynamics,[106-111,117,126] and the more rigorous TSH approach from the exact factorization of electronic-nuclear wavefunction.[30]

3.2. Azomethane

Azomethane is often used as a chemical source for radical generation since it can decompose into alkyl radicals and nitrogen after the absorption of ultraviolet light in the gas phase.[127] Previous theoretical studies with the FSSH and AIMS methods showed that azomethane would undergo an ultrafast nonadiabatic decay process after excitation.[119-120] As a typical system for benchmark, we chose azomethane to examine the SQC/MM dynamics.

For azomethane, only two states, S_1 and S_0, are involved in the nonadiabatic dynamics process in this work. When the systems are put in the S_1 state, most of the trajectories decay to the S_0 state within 350 fs for γ-adjusted SQC/MM dynamics, consistent with our own FSSH dynamics and previous AIMS dynamics.[119-120] While for the γ-fixed SQC/MM dynamics, about half of the

trajectories still stay at the S_1 state at 350 fs, see Figure 5(a). This phenomenon is very unlike that of $CH_2NH_2^+$, where the time-dependent electronic populations of S_1 of SQC/MM dynamics with both γ-adjusted and γ-fixed versions are very close (Figure 1).

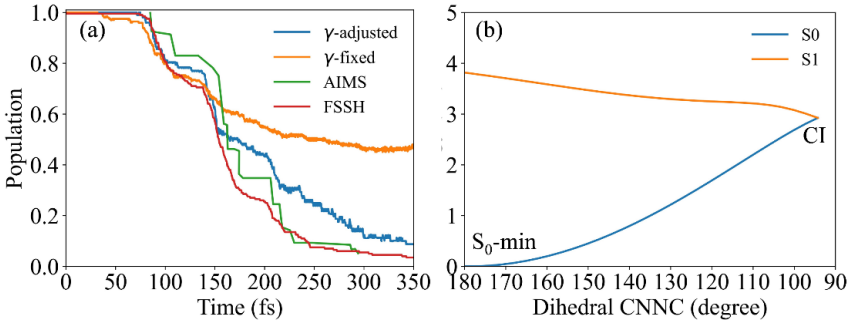

Figure 5. (a): Time-dependent electronic population of S_1 with different dynamics methods. 200 trajectories are used in the SQC/MM and FSSH dynamics. The results of the AIMS dynamics are taken from previous work.[119] (b) Linear interpolated potential energy curve from S_0 minimum to CI.

To understand the general feature of nonadiabatic dynamics of azomethane, we optimized the S_1/S_0 CI, and plotted the linear interpolated potential energy curve from S_0 minimum to CI, see Figure 5(b). Consistent with previous studies,[119] there is no barrier along the photoisomerization pathway.

Since the rotation of the central N-N double bond, characterized by the dihedral angle of CNNC, plays an important role in the nonadiabatic decay of azomethane, the time-dependent evolution of dihedral angle of CNNC for all trajectories of SQC/MM dynamics with γ-adjusted and γ-fixed is plotted, see Figure 6. The trajectories after the "switching points" are not plotted for

a better view of the trajectory propagation on the excited state from the Frank-Condon (FC) region to the S_1/S_0 CI.

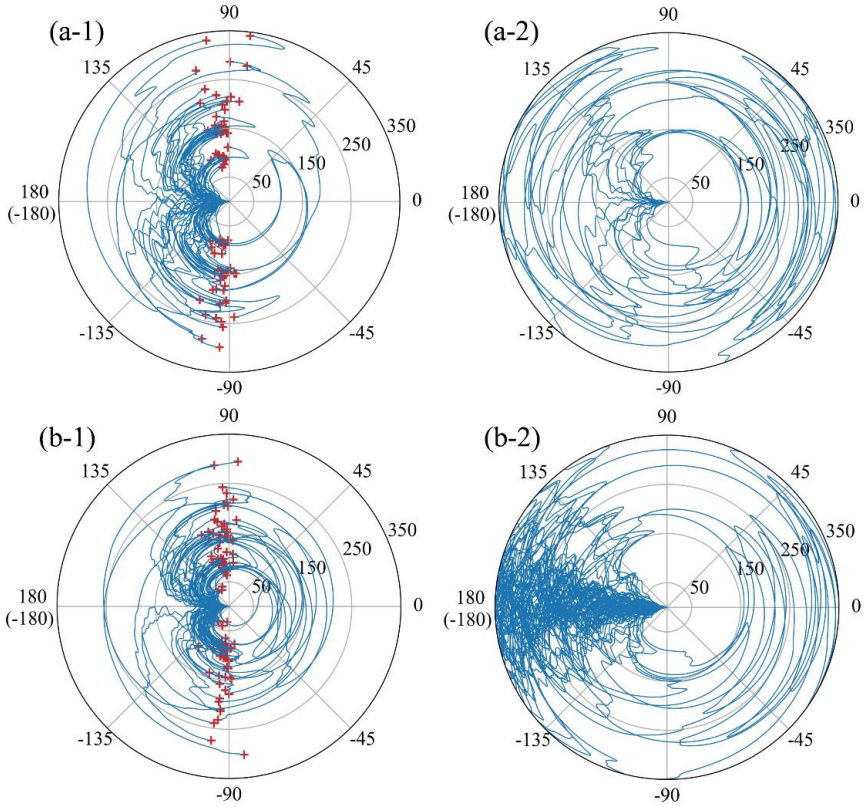

Figure 6. Time-dependent evolution of dihedral angle of CNNC for all trajectories before decaying to the S_0 of (a) γ-adjusted and (b) γ-fixed SQC/MM dynamics. The trajectories that decay and do not decay to the S_0 within 350 fs are shown in (1) and (2) separately. The red points indicate the "switching points" from S_1 to S_0. The radial and angular in the polar coordinates represent the time (fs) and dihedral angle (degree), respectively.

Clearly, the trajectory must experience a strong twisting motion of the CNNC dihedral angles if it goes to the ground state via the S_0/S_1 CI. Otherwise, the trajectory remains on the excited state, and no S_1 population decays observed. For the γ-adjusted dynamics, most trajectories show the

strong rotation of the NN double bond, and the trajectory access the geometries with a very small energy gap. This means that the majority of the trajectories follow the isomerization channels and decay to the ground state via the relevant CIs. While for γ-fixed dynamics, a large number of trajectories do not show the significant CNNC twisting motion, but display a oscillation of the CNNC angle around 180 (-180) degrees. These trajectories simply stay on the S_1 state and do not decay to the S_0 state at all.

Figure 5(b) shows that the energy of the S_0/S_1 CI is lower than that of S_1 at the S_0-min geometry. No energy barrier exists along the isomerization reaction pathway. Thus, the trajectory should naturally follow the barrierless pathway and access the S_0/S_1 CI without any doubt. However, for γ-fixed dynamics, a large number of trajectories seem to just stay in the S_1 state. The problematic feature can be explained by the fact that the nuclear motion is propagated by a kind of mean potential energy surface, instead of the S_1 state even before the trajectory reaches the CI. In γ-fixed dynamics, both S_1 and S_0 were involved in the nonadiabatic dynamics of azomethane, and the nuclear motion is governed by the effective potential

$$V_{eff} = n_0 E_0(\mathbf{R}) + n_1 E_1(\mathbf{R}) \tag{14}$$

where

$$\begin{aligned} n_0 &= \frac{1}{2}\left((x_0)^2 + (p_0)^2\right) - \gamma \\ n_1 &= \frac{1}{2}\left((x_1)^2 + (p_1)^2\right) - \gamma \end{aligned} \tag{15}$$

are time-dependent action variables of electronic states for each trajectory. Please notice that the effective potential on the nuclear part given in Eq. (14) is rather approximated when the

symmetrized form of the effective potential [Eq. (4)] is employed. However, the essential ideas behind them should be rather similar and thus we still can use Eq. (14-15) for the below discussions.

Certainly, the effective potential given in Eq. (14) defines the nuclear motion in the very beginning of the dynamics. Because both two action variables were obtained stochastically by sampling procedure, the effective potential is the linear combination of the S_0 and S_1 potential. As the consequence, the BO dynamics is not recovered for the single trajectory, while in principle the early-stage dynamics should follow the S_1 surface due to the negligible S_0/S_1 NAC in the FC region. In the azomethane, the ground state is a strong bonded state near the S_0-min geometry. If the contribution of the n_0 is large enough, the effective potential may become a bonded potential that prevents the trajectory escaping from the FC region. To clarify this idea, we plotted the initial sampled action variables and labeled their final assignment in Figure 7

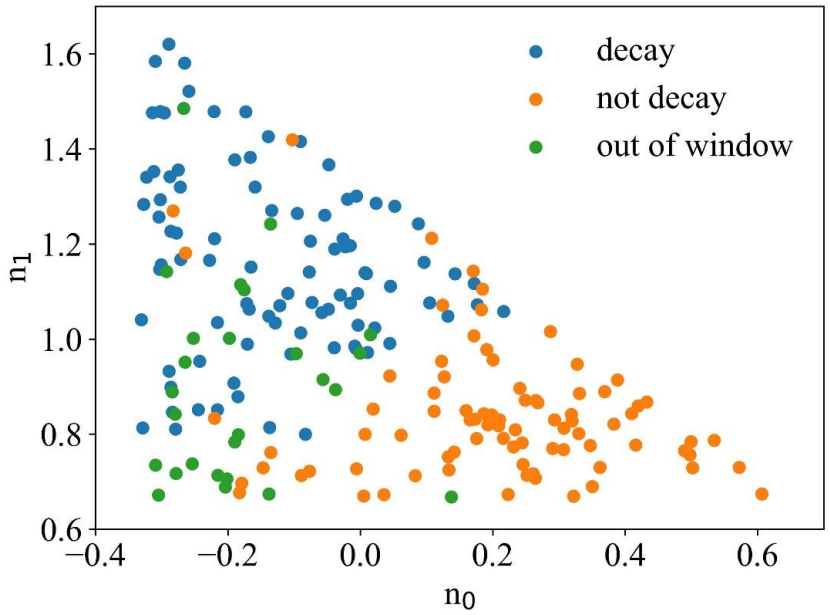

Figure 7. Distribution of the initial sample n_0 and n_1 of all trajectories for γ-fixed dynamics. The

labels ‘decay’ and ‘not decay’ mean the trajectory decays and does not decay to the ground state within 350 fs in the γ-fixed SQC/MM dynamics, respectively. The label ‘out of window’ means the action values of the trajectory are not in any triangle window at the end of dynamics.

It is clear that the trajectories are more likely to stay in the excited state when n_0 is large. In this condition, the effective PES might become bonded, and the trajectory cannot arrive at the CI region. This explains why many trajectories do not decay in Figure 5(a).

As a contrast, in the γ-adjusted situation, the ZPE correction value of each trajectory is determined by its own initial condition. In such a case, the early-time dynamics almost becomes the pure BO dynamics when the NAC is small enough under the large S_0-S_1 energy gap. In this way, most trajectories may follow the correct potential and access the CI. This explains the fast and completed population decay of the γ-adjusted SQC/MM dynamics in Figure 5(a).

Clearly, the γ-adjusted SQC/MM dynamics result is much closer to that of the AIMS dynamics in Figure 5(a),[119] we suggest that this γ-adjusted approach should always be used. In addition, this choice is consistent with physical insight. When the ground states and excited-state are well separated in the energy domain in the FC region, the early-time excited-state dynamics should essentially the BO dynamics due to the extremely weak NACs. Thus, the employment of the γ-adjusted approach allows the trajectory propagation to recover this limit. This avoids the possible deficiency of the effective potential acting on the nuclear propagation in the γ-fixed approach. This observation is consistent with the ideas by Cotton and Miller,[92] who strongly

suggested using the γ-adjusted approach in the study of the gas-phase photochemistry of the molecular systems without too many DoFs.

4. Conclusion

In this work, we tried to implement the on-the-fly SQC/MM dynamics. The SQC/MM dynamics formulism in the adiabatic representation provides a rather clear idea for the direct combination with the electronic structure calculations. We chose the $CH_2NH_2^+$ and azomethane as typical examples to examine the performance of the on-the-fly SQC/MM dynamics. The results show that all dynamical features of the nonadiabatic dynamics of $CH_2NH_2^+$ are well captured by the on-the-fly SQC/MM dynamics, no matter the γ-adjusted or γ-fixed approach is used. While for azomethane, the γ-adjusted SQC/MM dynamics performs much better than the γ-fixed SQC/MM dynamics. The reason is that the former one can recover the BO dynamics features at the beginning of the trajectory when the electronic states are far from each other, while the latter one always uses a kind of the mean PES. As a result, the γ-adjusted approach is strongly recommended to be used in all on-the-fly SQC/MM nonadiabatic dynamics.

This work demonstrates that the current on-the-fly SQC/MM dynamics provides a very promising approach to simulate the nonadiabatic dynamics of polyatomic molecules. When the MM Hamiltonian is considered, the SQC/MM dynamics is a simple dynamics approach, which serves as a zero-order approximation of more advanced semi-classical dynamics methods with the inclusion of quantum effects. Starting from the SQC/MM dynamics, it is possible to obtain other

sophisticated semi-classical methods with different accurate levels by introducing more quantum correction terms. Thus, the current implementation work provides a good starting point to cooperate with more rigorous semi-classical dynamics in the on-the-fly dynamics simulation.

Appendix A: Convergence test for the number of trajectories used in the SQC/MM dynamics

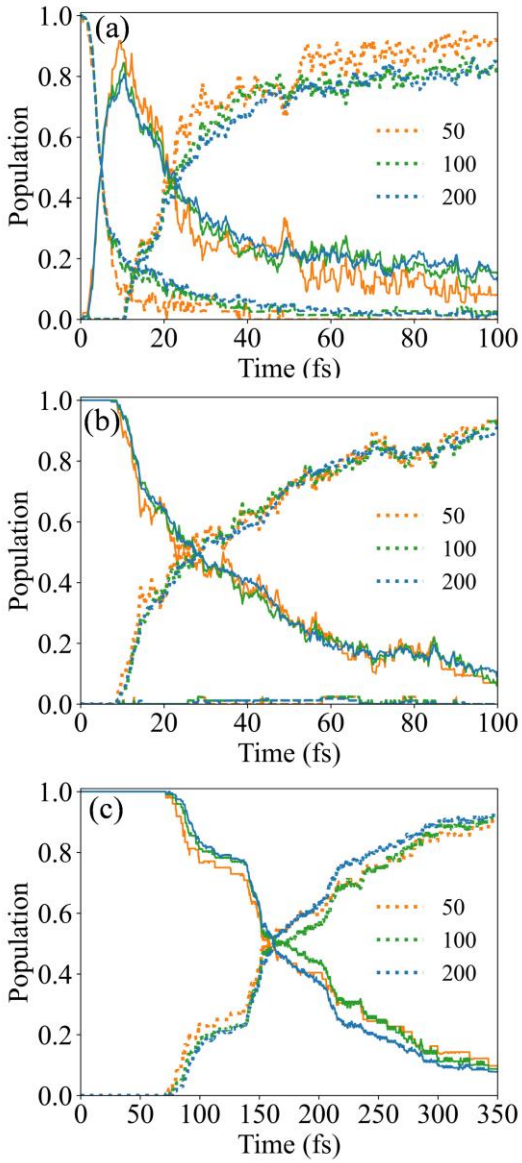

Figure A1. The time-dependent electronic population of S_0 (dotted line), S_1 (solid line) and S_2

(dashed line) states of SQC/MM dynamics for (a) $CH2NH2^+$ initial from S_2 state, (b) $CH2NH2^+$ initial from S_1 state and (c) azomethane initial from S_1 state. The number of trajectories is given in each subfigure. In the main text, 200 trajectories were used to discuss the results.

Author Information

Corresponding Author

E-mail: zhenggang.lan@m.scnu.edu.cn; zhenggang.lan@gmail.com.

Author Contributions

°Deping Hu and Yu Xie contributed equally to this work.

Notes

The authors declare no competing financial interest.

Acknowledgments

This work is supported by NSFC projects (No. 21933011, 21873112 and 21673266). The authors thank the Supercomputing Center, Computer Network Information Center, Chinese Academy of Sciences; National Supercomputing Center in Shenzhen for providing computational resources.

References

(1) Domcke, W.; Yarkony, D. R.; Köppel, H., *Conical intersections: Electronic structure, dynamics and spectroscopy*. World Scientic: 2004.

(2) Domcke, W.; Yarkony, D. R.; Köppel, H., *Conical intersections: Theory, computation and experiment*. World Scientific: 2011.

(3) May, V.; Kühn, O., *Charge and energy transfer dynamics in molecular systems*. Wiley-VCH Verlag GmbH & Co.: KGaA,Boschstr. 12, 69469 Weinheim, Germany, 2011.

(4) Schröter, M.; Ivanov, S. D.; Schulze, J.; Polyutov, S. P.; Yan, Y.; Pullerits, T.; Kühn, O. Exciton-vibrational coupling in the dynamics and spectroscopy of Frenkel excitons in molecular aggregates. *Phys. Rep.* **2015,** *567*, 1-78.

(5) Curchod, B. F. E.; Martínez, T. J. Ab initio nonadiabatic quantum molecular dynamics. *Chem. Rev.* **2018,** *118*, 3305-3336.

(6) Yonehara, T.; Hanasaki, K.; Takatsuka, K. Fundamental approaches to nonadiabaticity: Toward a chemical theory beyond the Born-Oppenheimer paradigm. *Chem. Rev.* **2012,** *112*, 499-542.

(7) Akimov, A. V.; Neukirch, A. J.; Prezhdo, O. V. Theoretical insights into photoinduced charge transfer and catalysis at oxide interfaces. *Chem. Rev.* **2013,** *113*, 4496-4565.

(8) Stock, G.; Thoss, M. Classical description of nonadiabatic quantum dynamics. *Adv. Chem. Phys.* **2005,** *131*, 243-375.

(9) Crespo-Otero, R.; Barbatti, M. Recent advances and perspectives on nonadiabatic mixed quantum-classical dynamics. *Chem. Rev.* **2018,** *118*, 7026-7068.

(10) Ben-Nun, M.; Martínez, T. J. Ab initio quantum molecular dynamics. *Adv. Chem. Phys.* **2002,** *121*, 439-512.

(11) Beck, M. H.; Jackle, A.; Worth, G. A.; Meyer, H. D. The multiconfiguration time-dependent Hartree (MCTDH) method: A highly efficient algorithm for propagating wavepackets. *Phys. Rep.* **2000,** *324*, 1-105.

(12) Wang, H. B.; Thoss, M. Multilayer formulation of the multiconfiguration time-dependent hartree theory. *J. Chem. Phys.* **2003,** *119*, 1289-1299.

(13) Yao, Y.; Sun, K.-W.; Luo, Z.; Ma, H. Full quantum dynamics simulation of a realistic molecular system using the adaptive time-dependent density matrix renormalization group method. *J. Phys. Chem. Lett.* **2018,** *9*, 413-419.

(14) Greene, S. M.; Batista, V. S. Tensor-train split-operator Fourier transform (TT-SOFT) method: Multidimensional nonadiabatic quantum dynamics. *J. Chem. Theory Comput.* **2017,** *13*, 4034-4042.

(15) Ren, J. J.; Shuai, Z. G.; Chan, G. K. L. Time-dependent density matrix renormalization group algorithms for nearly exact absorption and fluorescence spectra of molecular aggregates at both zero and finite temperature. *J. Chem. Theory Comput.* **2018,** *14*, 5027-5039.

(16) Li, X.; Tully, J. C.; Schlegel, H. B.; Frisch, M. J. Ab initio Ehrenfest dynamics. *J. Chem. Phys.* **2005,** *123*, 084106.

(17) Zhu, C. Y.; Jasper, A. W.; Truhlar, D. G. Non-Born-Oppenheimer trajectories with self-consistent decay of mixing. *J. Chem. Phys.* **2004,** *120*, 5543-5557.

(18) Tully, J. C. Molecular-dynamics with electronic-transitions. *J. Chem. Phys.* **1990,** *93*, 1061-1071.

(19) Subotnik, J. E.; Jain, A.; Landry, B.; Petit, A.; Ouyang, W. J.; Bellonzi, N. Understanding the surface hopping view of electronic transitions and decoherence. *Annu. Rev. Phys. Chem.* **2016,** *67*, 387-417.

(20) Wang, L. J.; Akimov, A.; Prezhdo, O. V. Recent progress in surface hopping: 2011-2015. *J. Phys. Chem. Lett.* **2016,** *7*, 2100-2112.

(21) Mai, S.; Marquetand, P.; González, L. Nonadiabatic dynamics: The SHARC approach. *Wiley Interdiscip. Rev.: Comput. Mol. Sci.* **2018,** *8*, e1370.

(22) Chen, H. T.; Reichman, D. R. On the accuracy of surface hopping dynamics in condensed phase non-adiabatic problems. *J. Chem. Phys.* **2016,** *144*, 094104.

(23) Granucci, G.; Persico, M.; Zoccante, A. Including quantum decoherence in surface hopping. *J. Chem. Phys.* **2010,** *133*, 134111.

(24) Zhu, C. Y.; Nobusada, K.; Nakamura, H. New implementation of the trajectory surface hopping method with use of the Zhu-Nakamura theory. *J. Chem. Phys.* **2001,** *115*, 3031-3044.

(25) Zimmermann, T.; Vaníček, J. Efficient on-the-fly ab initio semiclassical method for

computing time-resolved nonadiabatic electronic spectra with surface hopping or Ehrenfest dynamics. *J. Chem. Phys.* **2014,** *141*.

(26) Begušić, T.; Roulet, J.; Vaníček, J. On-the-fly ab initio semiclassical evaluation of time-resolved electronic spectra. *J. Chem. Phys.* **2018,** *149*.

(27) Persico, M.; Granucci, G. An overview of nonadiabatic dynamics simulations methods, with focus on the direct approach versus the fitting of potential energy surfaces. *Theor. Chem. Acc.* **2014,** *133*, 1526.

(28) Belyaev, A. K.; Lasser, C.; Trigila, G. Landau-Zener type surface hopping algorithms. *J. Chem. Phys.* **2014,** *140*, 224108.

(29) Granucci, G.; Persico, M. Critical appraisal of the fewest switches algorithm for surface hopping. *J. Chem. Phys.* **2007,** *126*, 134114.

(30) Ha, J.-K.; Lee, I. S.; Min, S. K. Surface hopping dynamics beyond nonadiabatic couplings for quantum coherence. *J. Phys. Chem. Lett.* **2018,** *9*, 1097-1104.

(31) Abedi, A.; Maitra, N. T.; Gross, E. K. U. Exact factorization of the time-dependent electron-nuclear wave function. *Phys. Rev. Lett.* **2010,** *105*, 123002.

(32) Richings, G. W.; Polyak, I.; Spinlove, K. E.; Worth, G. A.; Burghardt, I.; Lasorne, B. Quantum dynamics simulations using Gaussian wavepackets: The vMCG method. *Int. Rev. Phys. Chem.* **2015,** *34*, 269-308.

(33) Shalashilin, D. V. Quantum mechanics with the basis set guided by Ehrenfest trajectories: Theory and application to spin-boson model. *J. Chem. Phys.* **2009,** *130*, 244101.

(34) Makhov, D. V.; Symonds, C.; Fernandez-Alberti, S.; Shalashilin, D. V. Ab initio quantum direct dynamics simulations of ultrafast photochemistry with Multiconfigurational Ehrenfest approach. *Chem. Phys.* **2017,** *493*, 200-218.

(35) Symonds, C.; Kattirtzi, J. A.; Shalashilin, D. V. The effect of sampling techniques used in the multiconfigurational Ehrenfest method. *J. Chem. Phys.* **2018,** *148*, 184113.

(36) Meyer, H. D.; Miller, W. H. Classical analog for electronic degrees of freedom in non-

adiabatic collision processes. *J. Chem. Phys.* **1979,** *70*, 3214-3223.

(37) Cotton, S. J.; Miller, W. H. Symmetrical windowing for quantum states in quasi-classical trajectory simulations. *J. Phys. Chem. A* **2013,** *117*, 7190-7194.

(38) Miller, W. H.; Cotton, S. J. Classical molecular dynamics simulation of electronically non-adiabatic processes. *Faraday Discuss.* **2016,** *195*, 9-30.

(39) Stock, G.; Thoss, M. Semiclassical description of nonadiabatic quantum dynamics. *Phys. Rev. Lett.* **1997,** *78*, 578-581.

(40) Liu, J. A unified theoretical framework for mapping models for the multi-state Hamiltonian. *J. Chem. Phys.* **2016,** *145*, 204105.

(41) Sun, X.; Miller, W. H. Semiclassical initial value representation for electronically nonadiabatic molecular dynamics. *J. Chem. Phys.* **1997,** *106*, 6346-6353.

(42) Saller, M. A. C.; Kelly, A.; Richardson, J. O. On the identity of the identity operator in nonadiabatic linearized semiclassical dynamics. *J. Chem. Phys.* **2019,** *150*, 071101.

(43) Saller, M. A. C.; Kelly, A.; Richardson, J. O. Improved population operators for multi-state nonadiabatic dynamics with the mixed quantum-classical mapping approach. *Faraday Discuss.* **2020,** *221*, 150-167.

(44) He, X.; Liu, J. A new perspective for nonadiabatic dynamics with phase space mapping models. *J. Chem. Phys.* **2019,** *151*, 024105.

(45) Mulvihill, E.; Gao, X.; Liu, Y. D.; Schubert, A.; Dunietz, B. D.; Geva, E. Combining the mapping hamiltonian linearized semiclassical approach with the generalized quantum master equation to simulate electronically nonadiabatic molecular dynamics. *J. Chem. Phys.* **2019,** *151*, 074103.

(46) Liu, Y.; Gao, X.; Lai, Y.; Mulvihill, E.; Geva, E. Electronic dynamics through conical intersections via quasiclassical mapping Hamiltonian methods. *J. Chem. Theory Comput.* **2020,** *16*, 4479-4488.

(47) Gao, X.; Saller, M. A. C.; Liu, Y.; Kelly, A.; Richardson, J. O.; Geva, E. Benchmarking

quasiclassical mapping Hamiltonian methods for simulating electronically nonadiabatic molecular dynamics. *J. Chem. Theory Comput.* **2020,** *16*, 2883-2895.

(48) Gao, X.; Lai, Y.; Geva, E. Simulating absorption spectra of multiexcitonic systems via quasiclassical mapping Hamiltonian methods. *J. Chem. Theory Comput.* **2020,** *16*, 6465-6480.

(49) Gao, X.; Geva, E. A nonperturbative methodology for simulating multidimensional spectra of multiexcitonic molecular systems via quasiclassical mapping Hamiltonian methods. *J. Chem. Theory Comput.* **2020,** *16*, 6491-6502.

(50) Kim, H.; Nassimi, A.; Kapral, R. Quantum-classical Liouville dynamics in the mapping basis. *J. Chem. Phys.* **2008,** *129*, 084102.

(51) Kelly, A.; Rhee, Y. M. Mixed quantum-classical description of excitation energy transfer in a model Fenna-Matthews-Olsen complex. *J. Phys. Chem. Lett.* **2011,** *2*, 808-812.

(52) Kim, H. W.; Rhee, Y. M. Improving long time behavior of Poisson bracket mapping equation: A non-Hamiltonian approach. *J. Chem. Phys.* **2014,** *140*, 184106.

(53) Freedman, H.; Hanna, G. Mixed quantum-classical Liouville simulation of vibrational energy transfer in a model alpha-helix at 300 k. *Chem. Phys.* **2016,** *477*, 74-87.

(54) Bonella, S.; Coker, D. F. Semi-classical implementation of mapping Hamiltonian methods for general non-adiabatic problems. *Chem. Phys.* **2001,** *268*, 189-200.

(55) Bonella, S.; Coker, D. F. A semiclassical limit for the mapping hamiltonian approach to electronically nonadiabatic dynamics. *J. Chem. Phys.* **2001,** *114*, 7778-7789.

(56) Huo, P. F.; Coker, D. F. Consistent schemes for non-adiabatic dynamics derived from partial linearized density matrix propagation. *J. Chem. Phys.* **2012,** *137*, 22a535.

(57) Huo, P.; III, T. F. M.; Coker, D. F. Communication: Predictive partial linearized path integral simulation of condensed phase electron transfer dynamics. *J. Chem. Phys.* **2013,** *139*, 151103.

(58) Provazza, J.; Segatta, F.; Garavelli, M.; Coker, D. F. Semiclassical path integral calculation of nonlinear optical spectroscopy. *J. Chem. Theory Comput.* **2018,** *14*, 856-866.

(59) Ananth, N.; Miller, T. F. Exact quantum statistics for electronically nonadiabatic systems

using continuous path variables. *J. Chem. Phys.* **2010,** *133*, 234103.

(60) Tao, G. A multi-state trajectory method for non-adiabatic dynamics simulations. *J. Chem. Phys.* **2016,** *144*, 094108.

(61) Tao, G. H. Coherence-controlled nonadiabatic dynamics via state-space decomposition: A consistent way to incorporate Ehrenfest and Born-Oppenheimer-like treatments of nuclear motion. *J. Phys. Chem. Lett.* **2016,** *7*, 4335-4339.

(62) Liao, J.-L.; Voth, G. A. A centroid molecular dynamics approach for nonadiabatic dynamical processes in condensed phases: The spin-boson case. *J. Phys. Chem. B* **2002,** *106*, 8449-8455.

(63) Ananth, N. Mapping variable ring polymer molecular dynamics: A path-integral based method for nonadiabatic processes. *J. Chem. Phys.* **2013,** *139*, 124102.

(64) Pierre, S.; Duke, J. R.; Hele, T. J. H.; Ananth, N. A mapping variable ring polymer molecular dynamics study of condensed phase proton-coupled electron transfer. *J. Chem. Phys.* **2017,** *147*, 234103.

(65) Chowdhury, S. N.; Huo, P. Coherent state mapping ring polymer molecular dynamics for non-adiabatic quantum propagations. *J. Chem. Phys.* **2017,** *147*, 214109.

(66) Richardson, J. O.; Meyer, P.; Pleinert, M. O.; Thoss, M. An analysis of nonadiabatic ring-polymer molecular dynamics and its application to vibronic spectra. *Chem. Phys.* **2017,** *482*, 124-134.

(67) Richardson, J. O.; Thoss, M. Communication: Nonadiabatic ring-polymer molecular dynamics. *J. Chem. Phys.* **2013,** *139*, 031102.

(68) Ranya, S.; Ananth, N. Multistate ring polymer instantons and nonadiabatic reaction rates. *J. Chem. Phys.* **2020,** *152*, 114112.

(69) Chowdhury, S. N.; Huo, P. F. State dependent ring polymer molecular dynamics for investigating excited nonadiabatic dynamics. *J. Chem. Phys.* **2019,** *150*, 244102.

(70) Müller, U.; Stock, G. Flow of zero-point energy and exploration of phase space in classical simulations of quantum relaxation dynamics. II. Application to nonadiabatic processes. *J. Chem.*

Phys. **1999,** *111*, 77-88.

(71) Stock, G.; Müller, U. Flow of zero-point energy and exploration of phase space in classical simulations of quantum relaxation dynamics. *J. Chem. Phys.* **1999,** *111*, 65-76.

(72) Golosov, A. A.; Reichman, D. R. Classical mapping approaches for nonadiabatic dynamics: Short time analysis. *J. Chem. Phys.* **2001,** *114*, 1065-1074.

(73) Cotton, S. J.; Igumenshchev, K.; Miller, W. H. Symmetrical windowing for quantum states in quasi-classical trajectory simulations: Application to electron transfer. *J. Chem. Phys.* **2014,** *141*, 084104.

(74) Miller, W. H.; Cotton, S. J. Communication: Note on detailed balance in symmetrical quasi-classical models for electronically non-adiabatic dynamics. *J. Chem. Phys.* **2015,** *142*, 131103.

(75) Cotton, S. J.; Liang, R. B.; Miller, W. H. On the adiabatic representation of Meyer-Miller electronic-nuclear dynamics. *J. Chem. Phys.* **2017,** *147*, 064112.

(76) Jain, A.; Subotnik, J. E. Vibrational energy relaxation: A benchmark for mixed quantum-classical methods. *J. Phys. Chem. A* **2018,** *122*, 16-27.

(77) Bellonzi, N.; Jain, A.; Subotnik, J. E. An assessment of mean-field mixed semiclassical approaches: Equilibrium populations and algorithm stability. *J. Chem. Phys.* **2016,** *144*, 154110.

(78) Li, T. E.; Nitzan, A.; Sukharev, M.; Martínez, T.; Chen, H. T.; Subotnik, J. E. Mixed quantum-classical electrodynamics: Understanding spontaneous decay and zero-point energy. *Phys. Rev. A* **2018,** *97*, 032105.

(79) Kananenka, A. A.; Hsieh, C.-Y.; Cao, J.; Geva, E. Nonadiabatic dynamics via the symmetrical quasi-classical method in the presence of anharmonicity. *J. Phys. Chem. Lett.* **2017,** *9*, 319-326.

(80) Cotton, S. J.; Miller, W. H. A new symmetrical quasi-classical model for electronically non-adiabatic processes: Application to the case of weak non-adiabatic coupling. *J. Chem. Phys.* **2016,** *145*, 144108.

(81) Cotton, S. J.; Miller, W. H. The symmetrical quasi-classical model for electronically non-adiabatic processes applied to energy transfer dynamics in site-exciton models of light-harvesting

complexes. *J. Chem. Theory Comput.* **2016,** *12*, 983-991.

(82) Cotton, S. J.; Miller, W. H. Symmetrical windowing for quantum states in quasi-classical trajectory simulations: Application to electronically non-adiabatic processes. *J. Chem. Phys.* **2013,** *139*, 234112.

(83) Tao, G. Understanding electronically non-adiabatic relaxation dynamics in singlet fission. *J. Chem. Theory Comput.* **2015,** *11*, 28-36.

(84) Tao, G. Electronically nonadiabatic dynamics in singlet fission: A quasi-classical trajectory simulation. *J. Phys. Chem. C* **2014,** *118*, 17299-17305.

(85) Tao, G. Bath effect in singlet fission dynamics. *J. Phys. Chem. C* **2014,** *118*, 27258-27264.

(86) Liang, R.; Cotton, S. J.; Binder, R.; Hegger, R.; Burghardt, I.; Miller, W. H. The symmetrical quasi-classical approach to electronically nonadiabatic dynamics applied to ultrafast exciton migration processes in semiconducting polymers. *J. Chem. Phys.* **2018,** *149*, 044101.

(87) Xie, Y.; Zheng, J.; Lan, Z. Performance evaluation of the symmetrical quasi-classical dynamics method based on Meyer-Miller mapping Hamiltonian in the treatment of site-exciton models. *J. Chem. Phys.* **2018,** *149*, 174105.

(88) Sandoval_C., J. S.; Mandal, A.; Huo, P. Symmetric quasi-classical dynamics with quasi-diabatic propagation scheme. *J. Chem. Phys.* **2018,** *149*, 044115.

(89) Provazza, J.; Coker, D. F. Communication: Symmetrical quasi-classical analysis of linear optical spectroscopy. *J. Chem. Phys.* **2018,** *148*, 181102.

(90) Zheng, J.; Peng, J. W.; Xie, Y.; Long, Y. Z.; Ning, X.; Lan, Z. G. Study of the exciton dynamics in perylene bisimide (PBI) aggregates with symmetrical quasiclassical dynamics based on the Meyer-Miller mapping hamiltonian. *Phys. Chem. Chem. Phys.* **2020,** *22*, 18192-18204.

(91) Cotton, S. J.; Miller, W. H. A symmetrical quasi-classical windowing model for the molecular dynamics treatment of non-adiabatic processes involving many electronic states. *J. Chem. Phys.* **2019,** *150*, 104101.

(92) Cotton, S. J.; Miller, W. H. Trajectory-adjusted electronic zero point energy in classical

Meyer-Miller vibronic dynamics: Symmetrical quasiclassical application to photodissociation. *J. Chem. Phys.* **2019,** *150*, 194110.

(93) Zheng, J.; Xie, Y.; Jiang, S. s.; Long, Y. z.; Ning, X.; Lan, Z. G. Ultrafast electron transfer with symmetrical quasi-classical dynamics based on mapping hamiltonian and quantum dynamics based on ml-mctdh. *Chin. J. Chem. Phys.* **2017,** *30*, 800-810.

(94) Mandal, A.; Sandoval C, J. S.; Shakib, F. A.; Huo, P. Quasi-diabatic propagation scheme for direct simulation of proton-coupled electron transfer reaction. *J. Phys. Chem. A* **2019,** *123*, 2470-2482.

(95) Mandal, A.; Yamijala, S.; Huo, P. F. Quasi-diabatic representation for nonadiabatic dynamics propagation. *J. Chem. Theory Comput.* **2018,** *14*, 1828-1840.

(96) Mandal, A.; Shakib, F. A.; Huo, P. Investigating photoinduced proton coupled electron transfer reaction using quasi diabatic dynamics propagation. *J. Chem. Phys.* **2018,** *148*, 244102.

(97) Zhou, W.; Mandal, A.; Huo, P. Quasi-diabatic scheme for nonadiabatic on-the-fly simulations. *J. Phys. Chem. Lett.* **2019,** *10*, 7062-7070.

(98) Mead, C. A.; Truhlar, D. G. Conditions for the Definition of a Strictly Diabatic Electronic Basis for Molecular-Systems. *J. Chem. Phys.* **1982,** *77*, 6090-6098.

(99) McLachlan, A. The wave functions of electronically degenerate states. *Mol. Phys.* **1961,** *4*, 417-423.

(100) Pacher, T.; Mead, C. A.; Cederbaum, L. S.; Koppel, H. Gauge-theory and quasidiabatic states in molecular physics. *J. Chem. Phys.* **1989,** *91*, 7057-7062.

(101) Baer, M. Adiabatic and diabatic representations for atom-molecule collisions: Treatment of the collinear arrangement. *Chem. Phys. Lett.* **1975,** *35*, 112-118.

(102) Ananth, N.; Venkataraman, C.; Miller, W. H. Semiclassical description of electronically nonadiabatic dynamics via the initial value representation. *J. Chem. Phys.* **2007,** *127*, 084114.

(103) Coker, D. F.; Bonella, S., Linearized nonadiabatic dynamics in the adiabatic representation. In *Springer Ser Chem Ph*, 2007; pp 321-340.

(104) Hsieh, C.-Y.; Schofield, J.; Kapral, R. Forward–backward solution of quantum-classical Liouville equation in the adiabatic mapping basis. *Mol. Phys.* **2013,** *111*, 3546-3554.

(105) Tang, D. D.; Fang, W. H.; Shen, L.; Cui, G. L. Combining Meyer-Miller hamiltonian with electronic structure methods for on-the-fly nonadiabatic dynamics simulations: Implementation and application. *Phys. Chem. Chem. Phys.* **2019,** *21*, 17109-17117.

(106) Du, L. K.; Lan, Z. G. Correction to "an on-the-fly surface-hopping program JADE for nonadiabatic molecular dynamics of polyatomic systems: Implementation and applications". *J. Chem. Theory Comput.* **2015,** *11*, 4522-4523.

(107) Du, L. K.; Lan, Z. G. An on-the-fly surface-hopping program JADE for nonadiabatic molecular dynamics of polyatomic systems: Implementation and applications. *J. Chem. Theory Comput.* **2015,** *11*, 1360-1374.

(108) Fabiano, E.; Keal, T. W.; Thiel, W. Implementation of surface hopping molecular dynamics using semiempirical methods. *Chem. Phys.* **2008,** *349*, 334-347.

(109) Hollas, D.; Šištík, L.; Hohenstein, E. G.; Martínez, T. J.; Slavíček, P. Nonadiabatic ab initio molecular dynamics with the floating occupation molecular orbital-complete active space configuration interaction method. *J. Chem. Theory Comput.* **2018,** *14*, 339-350.

(110) Barbatti, M.; Aquino, A. J. A.; Lischka, H. Ultrafast two-step process in the non- adiabatic relaxation of the CH2NH2+ molecule. *Mol. Phys.* **2006,** *104*, 1053-1060.

(111) Barbatti, M.; Granucci, G.; Persico, M.; Ruckenbauer, M.; Vazdar, M.; Eckert-Maksić, M.; Lischka, H. The on-the-fly surface-hopping program system NEWTON-X: Application to ab initio simulation of the nonadiabatic photodynamics of benchmark systems. *J. Photoch. Photobio. A* **2007,** *190*, 228-240.

(112) Kunisada, T.; Ushiyama, H.; Yamashita, K. A new implementation of ab initio Ehrenfest dynamics using electronic configuration basis: Exact formulation with molecular orbital connection and effective propagation scheme with locally quasi-diabatic representation. *Int. J. Quantum Chem.* **2016,** *116*, 1205-1213.

(113) Kunisada, T.; Ushiyama, H.; Yamashita, K. Electron wavepacket approaches to non-adiabatic transition processes in the internal rotational motion of H2CNH2+- charge oscillation due to electronic coherence. *Chem. Phys. Lett.* **2015,** *635*, 345-349.

(114) Fischer, M.; Handt, J.; Schmidt, R. Nonadiabatic quantum molecular dynamics with hopping. III. Photoinduced excitation and relaxation of organic molecules. *Phys. Rev. A* **2014,** *90*, 012527.

(115) West, A. C.; Barbatti, M.; Lischka, H.; Windus, T. L. Nonadiabatic dynamics study of methaniminium with ORMAS: Challenges of incomplete active spaces in dynamics simulations. *Comput. Theor. Chem.* **2014,** *1040*, 158-166.

(116) Zimmermann, T.; Vanicek, J. Evaluation of the importance of spin-orbit couplings in the nonadiabatic quantum dynamics with quantum fidelity and with its efficient "on-the-fly" ab initio semiclassical approximation. *J. Chem. Phys.* **2012,** *137*, 22A516.

(117) Tavernelli, I.; Tapavicza, E.; Rothlisberger, U. Non-adiabatic dynamics using time-dependent density functional theory: Assessing the coupling strengths. *J. Mol. Struct.* **2009,** *914*, 22-29.

(118) Fabiano, E.; Groenhof, G.; Thiel, W. Approximate switching algorithms for trajectory surface hopping. *Chem. Phys.* **2008,** *351*, 111-116.

(119) Gaenko, A.; DeFusco, A.; Varganov, S. A.; Martínez, T. J.; Gordon, M. S. Interfacing the ab initio multiple spawning method with electronic structure methods in GAMESS: Photo-decay of trans-azomethane. *J. Phys. Chem. A* **2014,** *118*, 10902-10908.

(120) Sellner, B.; Ruckenbauer, M.; Stambolic, I.; Barbatti, M.; Aquino, A. J.; Lischka, H. Photodynamics of azomethane: A nonadiabatic surface-hopping study. *J. Phys. Chem. A* **2010,** *114*, 8778-8785.

(121) Frisch, M. J.; Trucks, G. W.; Schlegel, H. B.; Scuseria, G. E.; Robb, M. A.; Cheeseman, J. R.; Scalmani, G.; Barone, V.; Petersson, G. A.; Nakatsuji, H.; Li, X.; Caricato, M.; Marenich, A. V.; Bloino, J.; Janesko, B. G.; Gomperts, R.; Mennucci, B.; Hratchian, H. P.; Ortiz, J. V.; Izmaylov, A. F.; Sonnenberg, J. L.; Williams; Ding, F.; Lipparini, F.; Egidi, F.; Goings, J.; Peng, B.; Petrone,

A.; Henderson, T.; Ranasinghe, D.; Zakrzewski, V. G.; Gao, J.; Rega, N.; Zheng, G.; Liang, W.; Hada, M.; Ehara, M.; Toyota, K.; Fukuda, R.; Hasegawa, J.; Ishida, M.; Nakajima, T.; Honda, Y.; Kitao, O.; Nakai, H.; Vreven, T.; Throssell, K.; Montgomery Jr., J. A.; Peralta, J. E.; Ogliaro, F.; Bearpark, M. J.; Heyd, J. J.; Brothers, E. N.; Kudin, K. N.; Staroverov, V. N.; Keith, T. A.; Kobayashi, R.; Normand, J.; Raghavachari, K.; Rendell, A. P.; Burant, J. C.; Iyengar, S. S.; Tomasi, J.; Cossi, M.; Millam, J. M.; Klene, M.; Adamo, C.; Cammi, R.; Ochterski, J. W.; Martin, R. L.; Morokuma, K.; Farkas, O.; Foresman, J. B.; Fox, D. J. *Gaussian 16 Rev. C.01*, Wallingford, CT, 2016.

(122) Werner, H. J.; Knowles, P. J. A second order multiconfiguration SCF procedure with optimum convergence. *J. Chem. Phys.* **1985,** *82*, 5053-5063.

(123) Knowles, P. J.; Werner, H.-J. An efficient second-order MCSCF method for long configuration expansions. *Chem. Phys. Lett.* **1985,** *115*, 259-267.

(124) Werner, H. J.; Knowles, P. J.; Knizia, G.; Manby, F. R.; Schutz, M. *Molpro, version 2012.1, a package of ab initio programs*, 2012.

(125) Barbatti, M.; Ruckenbauer, M.; Plasser, F.; Pittner, J.; Granucci, G.; Persico, M.; Lischka, H. Newton-X: A surface-hopping program for nonadiabatic molecular dynamics. *Wiley Interdisciplinary Reviews-Computational Molecular Science* **2014,** *4*, 26-33.

(126) Tapavicza, E.; Tavernelli, I.; Rothlisberger, U. Trajectory surface hopping within linear response time-dependent density-functional theory. *Phys. Rev. Lett.* **2007,** *98*, 023001.

(127) Diau, E. W.; Zewail, A. H. Femtochemistry of trans-azomethane: a combined experimental and theoretical study. *Chemphyschem* **2003,** *4*, 445-56.